INSTITUTE OF PHYSICS PUBLISHING EUROPEAN JOURNAL OF PHYSICS

Eur. J. Phys. **27** (2006) 109–118 doi:10.1088/0143-0807/27/1/012

Oriental magic mirrors and the Laplacian image

M V Berry

H H Wills Physics Laboratory, Tyndall Avenue, Bristol BS8 1TL, UK

Received 26 September 2005, in final form 20 October 2005
Published 24 November 2005
Online at stacks.iop.org/EJP/27/109

Abstract

The pattern embossed on the back of an oriental magic mirror appears in the patch of light projected onto a screen from its apparently featureless reflecting surface. In reality, the embossed pattern is reproduced in low relief on the front, and analysis shows that the projected image results from pre-focal ray deviation. In this interesting regime of geometrical optics, the image intensity is given simply by the Laplacian of the height function of the relief. For patterns consisting of steps, this predicts a characteristic effect, confirmed by observation: the image of each step exhibits a bright line on the low side and a dark line on the high side. Laplacian-image analysis of a magic-mirror image indicates that steps on the reflecting surface are about 400 nm high and laterally smoothed by about 0.5 mm.

1. Introduction

Cast and polished bronze mirrors, made in China and Japan for several thousand years, exhibit a curious property [1–4], long regarded as magical. A pattern embossed on the back (figure 1(b)) is visible in the patch of light projected onto a screen from the reflecting face (figure 2), when this is illuminated by a small source, even though no trace of the pattern can be discerned by direct visual inspection of the reflecting face (figure 1(a)). The pattern on the screen is not the result of the focusing responsible for conventional image formation, because its sharpness is independent of distance, and also because the magic mirrors are slightly convex. It was established long ago [2] that the effect results from the deviation of rays by weak undulations on the reflecting surface, introduced during the manufacturing process and too weak to see directly, that reproduce the much stronger relief embossed on the back. Such 'Makyoh imaging' (from the Japanese for 'wonder mirror') has been applied to detect small asperities on nominally flat semiconductor surfaces [5–8].

My aim here is to draw attention (section 2) to a simple and beautiful fact, central to the optics of magic mirrors, that has not been emphasized—either in the qualitative accounts [9–11] or in an extensive geometrical-optics analysis [12]: in the optical regime relevant to magic mirrors, the image intensity is given, in terms of the height function $h(\mathbf{r})$ of the relief

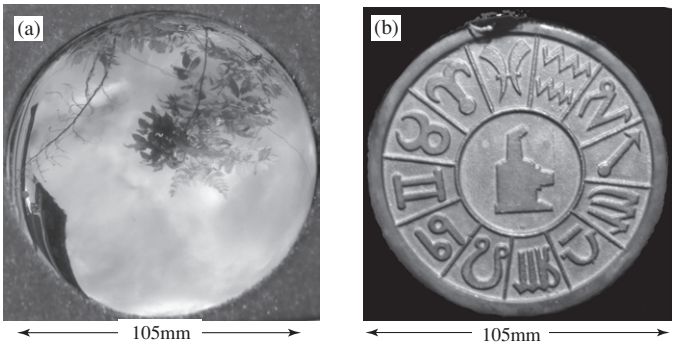

Figure 1. (a) Convex reflecting face of magic mirror, (b) pattern embossed on back face of magic mirror. These and subsequent images were photographed with a Fuji 610F digital camera, and saved as jpeg files, the only manipulation being conversion from RGB to greyscale.

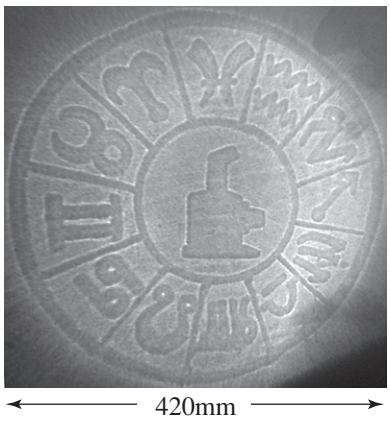

Figure 2. Magnified magic-mirror image reflected onto a screen by the illuminated front face.

on the reflecting surface, by the Laplacian $\nabla^2 h(\mathbf{r})$ (here $\mathbf{r}$ denotes position in the mirror plane: $\mathbf{r} = \{x, y\}$). The Laplacian image predicts striking effects for patterns, such as those on magic mirrors, that consist of steps (section 3); these predictions are supported by experiment (section 4). The detailed study of reflection from steps throws up an unresolved problem (section 5) concerning the relation between the pattern embossed on the back and the relief on the reflecting surface.

The Laplacian image is an approximation to geometrical optics, which is itself an approximation to physical optics. The appendix contains a discussion of the Laplacian image starting from the wave integral representing Fresnel diffraction from the mirror surface.

2. Geometrical optics and the Laplacian image

If we measure the height $h(\mathbf{r}')$ from the convex surface of the mirror (figure 3), assumed to have radius of curvature R_0, then the deviation of the surface undulations from a reference plane (figure 3) is

$$\eta(\mathbf{r}') = -\frac{r'^2}{2R_0} + h(\mathbf{r}'). \tag{1}$$

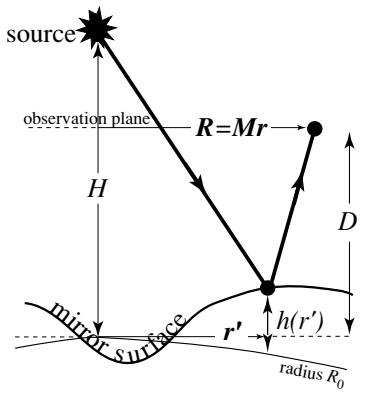

Figure 3. Geometry and coordinates for formation of magic-mirror image. For clarity, the surface elevation $h(\mathbf{r}')$ (measured from the convex surface with radius of curvature R_0) is exaggerated; in reality, the surface radii of curvature can be comparable with or smaller than R_0, so the mirror's undulating surface can be entirely convex.

The specularly reflected rays of geometrical optics are determined by the stationary value(s) of the optical path length L from the source (distance H from the reference plane) to the position $\mathbf{R}$ on the screen (distance D from the reference plane) via the point $\mathbf{r}'$ on the mirror. This is

$$\begin{aligned} L &= \sqrt{(H-\eta(\mathbf{r}'))^2 + r'^2} + \sqrt{(D-\eta(\mathbf{r}'))^2 + (\mathbf{R}-\mathbf{r}')^2} \\ &\approx H + D + \Lambda(\mathbf{r}', \mathbf{R}), \end{aligned} \tag{2}$$

where in the second line we have employed the paraxial approximation (all ray angles small), with

$$\Lambda(\mathbf{r}', \mathbf{R}) = \frac{r'^2}{2H} + \frac{(\mathbf{R}-\mathbf{r}')^2}{2D} + \frac{r'^2}{R_0} - 2h(\mathbf{r}'). \tag{3}$$

In applying the stationarity condition

$$\nabla_{\mathbf{r}'}\Lambda(\mathbf{r}', \mathbf{R}) = 0, \tag{4}$$

it is convenient to define the magnification M, the reduced distance Z, and the demagnified observation position $\mathbf{r}$ referred to the mirror surface:

$$M \equiv 1 + \frac{D}{H} + \frac{2D}{R_0}, \qquad Z \equiv \frac{2D}{M}, \qquad \mathbf{r} \equiv \frac{\mathbf{R}}{M}. \tag{5}$$

We note an effect of the convexity that will be important later: as the source and screen distance increase, Z approaches the finite asymptotic value R_0.

With these variables, the position $\mathbf{r}'(\mathbf{r},Z)$, on the mirror, of rays reaching the screen position $\mathbf{r}$, is the solution of

$$\mathbf{r} = \mathbf{r}' - Z\nabla h(\mathbf{r}'). \tag{6}$$

The focusing and defocusing responsible for the varying light intensity at $\mathbf{r}$ involves the Jacobian determinant of the transformation from $\mathbf{r}'$ to $\mathbf{r}$, giving, after a short calculation,

$$\begin{aligned} I_{\text{geom}}(\mathbf{r}, Z) &= \text{constant} \times \left(\frac{\partial x}{\partial x'}\frac{\partial y}{\partial y'} - \frac{\partial x}{\partial y'}\frac{\partial y}{\partial x'} \right)^{-1}_{\mathbf{r}'\to\mathbf{r}'(\mathbf{r},Z)} \\ &= \left(1 - Z\nabla^2 h(\mathbf{r}') + Z^2 \left(\frac{\partial h(\mathbf{r}')}{\partial x'^2}\frac{\partial h(\mathbf{r}')}{\partial y'^2} - \left(\frac{\partial h(\mathbf{r}')}{\partial x'\partial y'} \right)^2 \right) \right)^{-1}_{\mathbf{r}'\to\mathbf{r}'(\mathbf{r},Z)}, \end{aligned} \tag{7}$$

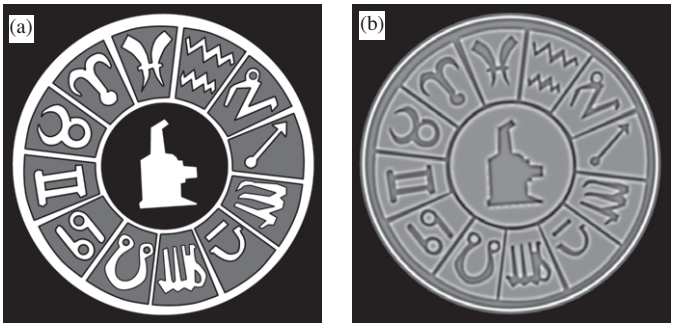

Figure 4. (a) Tracing of relief on the back of the mirror, with step heights shaded according to elevation (lowest black, highest white); (b) Laplacian image of (a), smoothed by $l = 0.5$ mm according to equations (10), (12) and (13).

where the result has been normalized to $I_{\text{geom}} = 1$ for the convex mirror without surface relief (i.e. $h(\mathbf{r}) = 0$).

So far, this is standard geometrical optics [12]. In general, more than one ray can reach $\mathbf{r}$—that is, (6) can have several solutions $\mathbf{r}'$—and the boundaries of regions reached by different numbers of rays are caustics [13, 14]. In magic mirrors, however, we are concerned with a limiting regime satisfying

$$\frac{Z}{R_{\text{min}}} \ll 1, \tag{8}$$

where R_{min} is the smallest radius of curvature of the surface irregularities. Then there is only one ray, (6) simplifies to

$$\mathbf{r}' \approx \mathbf{r}, \tag{9}$$

and the intensity simplifies to

$$I_{\text{Laplacian}}(\mathbf{r}, Z) = 1 + Z\nabla^2 h(\mathbf{r}). \tag{10}$$

This is the Laplacian image. Changing Z affects only the contrast of the image and not its form, so (10) explains why the sharpness of the image is independent of screen position, provided (8) holds. The intensity is a linear function of the surface irregularities h, which is not the case in general geometrical optics (i.e. when (8) is violated), where, as has been emphasized [12] the relation (7) is nonlinear. And, as already noted, for a distant source and screen Z approaches the value R_0, implying that (8) holds for any distance of the screen if $R_0 \ll R_{\text{min}}$, that is, provided the irregularities are sufficiently gentle or the mirror is sufficiently convex. Alternatively stated, the convexity of the mirror can compensate any concavity of the irregularity h, in which case there are no caustics for any screen position.

3. Laplacian images of steps

The relief h_{back} on the back of magic mirrors commonly consists of a pattern of steps (h_{back}, like h, is measured outwards from the mid-plane of the mirror, so increasing step heights on both the front and back correspond to increasing h and h_{back}). Figure 4(a) shows a tracing of the pattern of figure 1(b), with step heights shaded according to elevation. It seems that

during the manufacturing process this is reproduced on the reflecting surface, with the steps greatly diminished—by a factor a, say—and slightly smoothed—by a distance l, say—so that, modelling the smoothing as Gaussian,

$$h(\mathbf{r}', l) = \frac{a}{2\pi l^2} \iint \mathrm{d}^2\mathbf{r}''\, h_{\mathrm{back}}(\mathbf{r}'') \exp\left\{-\frac{(\mathbf{r}'' - \mathbf{r}')^2}{2l^2}\right\}. \tag{11}$$

Then the Laplacian image can be implemented with the transformation

$$\nabla^2 h(\mathbf{r}', l) = \iint \mathrm{d}^2\mathbf{r}''\, h_{\mathrm{back}}(\mathbf{r}'') K(\mathbf{r}'' - \mathbf{r}'), \tag{12}$$

where the kernel is

$$K(\mathbf{r}'' - \mathbf{r}') = \frac{a}{2\pi l^6}[(\mathbf{r}'' - \mathbf{r}')^2 - 2l^2] \exp\left\{-\frac{(\mathbf{r}'' - \mathbf{r}')^2}{2l^2}\right\}. \tag{13}$$

(In image processing, this transformation is commonly employed for edge detection [15–17].)

It is easy to implement the Laplacian image (10) using the transformation (12) and (13). In Mathematica$^{\mathrm{TM}}$, for example [18], this involves essentially only three lines of code: one to import the image as a list, one to define the kernel K, and one to define the convolution. Figure 4(b) shows a magic-mirror image simulated in this way; it should be compared with the observation in figure 2. The essential features of the image, correctly reproduced by the theory, are associated with the steps: each step on the back appears in the image as a bright line on the low side, where the concavity of h leads to a concentration of rays, and a dark line on the high side, where the convexity of h leads to a depletion of rays.

To examine the image in more detail, we model the l-smoothed step, with height h_0, by

$$h(x) = \frac{h_0}{2} \operatorname{erf}\left(\frac{x}{l}\right) = \frac{h_0}{\sqrt{\pi}} \int_0^{x/l} \mathrm{d}t \exp(-t^2) \tag{14}$$

and introduce the dimensionless position and distance variables

$$\xi \equiv \frac{x}{Ml}, \qquad \xi' \equiv \frac{x'}{l}, \qquad \zeta \equiv Z\frac{h_0}{l^2}. \tag{15}$$

Then the exact ray equation (6) becomes

$$\xi = \xi' - \frac{\zeta}{\sqrt{\pi}} \exp(-\xi'^2) \Rightarrow \xi'(\xi, \zeta), \tag{16}$$

and the geometrical intensity is

$$I_{\mathrm{geom}}(\xi, \zeta) = \left[1 + \frac{2\zeta\xi'}{\sqrt{\pi}} \exp\{-\xi'(\xi, \zeta)^2\}\right]^{-1}. \tag{17}$$

The Laplacian image (10) is simply

$$I_{\mathrm{Laplacian}}(\xi, \zeta) = 1 - \frac{2\zeta\xi}{\sqrt{\pi}} \exp\{-\xi^2\}. \tag{18}$$

4. Experiment

Equation (18) is the prediction of the Laplacian theory for the image of a smoothed step. To compare it with observation, we first extract a part of the image (figure 2), corresponding to a prominent step; this is shown in figure 5(a). Next, we reduce the noise by smoothing along the step (figure 5(b)). The intensity profile of the image is the full curve in figure 6.

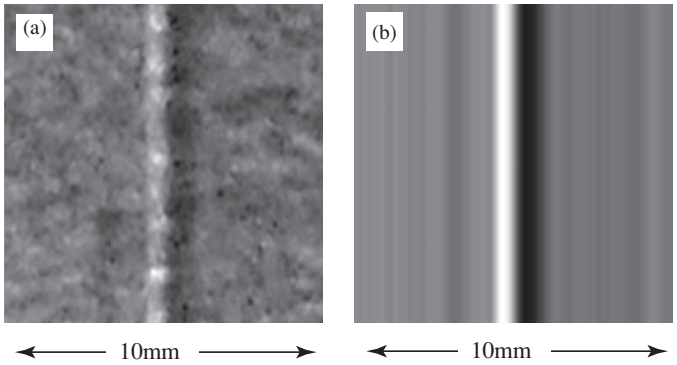

Figure 5. (a) Magnification of part of left-hand vertical step near the centre of magic-mirror image in figure 2; (b) as (a), after averaging along the step. The length scales denote distances on the mirror surface, not the image.

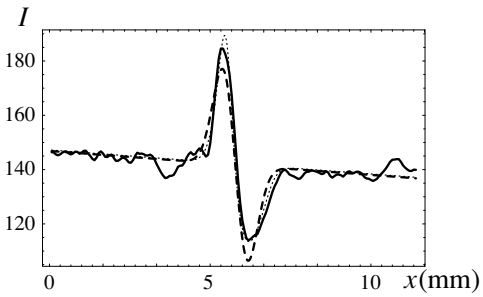

Figure 6. Full curve: intensity across the step in figure 5(b) (arbitrary units); dashed curve: Laplacian-image fit from equation (18), with a straight line of finite slope replacing the constant term; dotted curve: full geometrical-optics fit, incorporating the ray displacement (16) and intensity (17).

Measurements on the curve give the intensity contrast as

$$C_{\text{exp}} \equiv \frac{2(I_{\text{max}} - I_{\text{min}})}{(I_{\text{max}} + I_{\text{min}})} = 0.467. \tag{19}$$

Comparison with the theoretical contrast from the extrema of (18) (at $\xi = \pm 1/\sqrt{2}$), namely

$$C_{\text{theory}} = 2\zeta\sqrt{\frac{2}{\pi\,\mathrm{e}}}, \tag{20}$$

leads to the identification $\zeta = 0.482$.

In the experiment, the source (a halogen lamp) and screen were at the same distance from the mirror, also chosen to coincide with R_0: $D = H = R_0 = 800$ mm. Thus, from (5), and also as observed (cf the scale in figure 2), the magnification is $M = 4$, leading to $Z = H/2 = 400$ mm. Fitting the observed step profile to (18) (dashed curve in figure 6), gives the step width $l = 0.560$ mm. The relation (15) now gives the step height $h_0 = \zeta l^2/Z = 378$ nm. This value is substantially less than the wavelengths of visible light, so it is not surprising that the steps cannot be seen directly.

The Laplacian-image fit in figure 6 is good, but fails to incorporate a slight asymmetry between the two sides of the step: on the bright side, the intensity rises higher above the mean than it falls below the mean on the dark side. To understand this, we investigate the degree to which the condition (8) is satisfied. In the dimensionless variables (15), (8) corresponds to

$$\zeta \ll \zeta^* \equiv \sqrt{\frac{\pi\,\mathrm{e}}{2}} = 2.067\ldots \tag{21}$$

The value $\zeta = 0.482$ derived from observation is substantially smaller than ζ^*—well within the no-caustic regime that we have identified as corresponding to magic mirror imaging. However, fitting with the full geometrical-optics theory (16) and (17) (dotted curve in figure 6) gives a small correction that reduces the discrepancy by introducing an asymmetry in the correct sense. (The asymmetry between the bright and dark sides of the step increases with ζ until $\zeta = \zeta^*$ where the caustic is born.)

5. Concluding remarks

The theory based on the Laplacian image accords well with observation, at least for the mirror studied here. The key insight is that the image of a step is neither a dark line nor a bright line, as sometimes reported [11], but is bright on one side and dark on the other. It is possible that there are different types of magic mirror, where for example the relief is etched directly onto the reflecting surface and protected by a transparent film [11], but these do not seem to be common. Sometimes, the pattern reflected onto a screen is different from that on the back, but this is probably a trick, achieved by attaching a second layer of bronze, differently embossed, to the back of the mirror.

Pre-focal ray concentrations leading to Laplacian images are familiar in other contexts, though they are not always recognized as such. An example based on refraction occurs in old windows, where a combination of age and poor manufacture has distorted the glass. The distortion is not evident in views seen through the window when standing close to it. However, when woken by the low morning sun shining through a gap in the curtains onto an opposite wall, one often sees the distortions magnified as a pattern of irregular bright and dark lines. If the equivalent of (8) is satisfied, that is if the distortions and propagation distance are not too large, the intensity is the Laplacian image of the window surface. (When the condition is not satisfied, the distortions can generate caustics.)

Only the optics of the mirror has been studied here. The manner in which the pattern embossed on the back gets reproduced on the front has not been considered. Referring to (11), this involves the sign of the coefficient a in the relation between h_{back} and h. There have been several speculations about the formation of the relief. One is that the relief is generated while the mirror is cooling, by unequal contraction of the thick and thin parts of the pattern [10]; it is not clear what sign of a this leads to. Another [4] is that cooling generates stresses, and that during vigorous grinding and polishing the thin parts yield more than the thick parts, leading to the thick parts being worn down more; this leads to $a < 0$. However, this seems to contradict the observations, which point firmly to $a > 0$: bright (dark) lines on the image, indicating low (high) sides of the steps on the reflecting face, are associated with the low (high) sides of the steps on the back (figure 7(a)), not the reverse (figure 7(b)). This suggests two avenues for further research. First, the sign of a should be determined by direct measurement of the profile of the reflecting surface; I predict $a > 0$. Second, whatever the result, the mechanism should be investigated by which the process of manufacture reproduces onto the reflecting surface the pattern on the back.

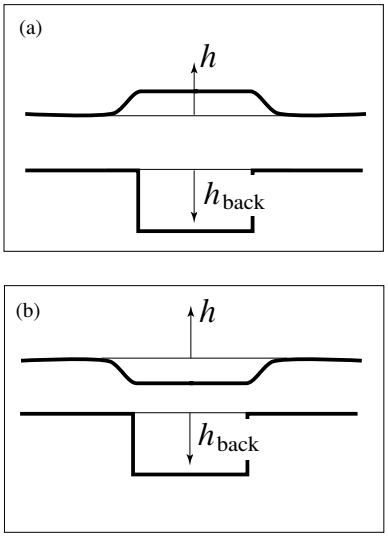

Figure 7. (a) Relief h of the reflecting surface with the same sign as the relief h_{back} embossed on the back, i.e. $a > 0$ in (11); this is the sign supported by observation. (b) As (a), but with $a < 0$, suggested by the stress-release theory but not by observation.

Acknowledgment

My research is supported by the Royal Society of London.

Appendix. Diffraction

For magic mirrors, the Laplacian-image intensity (10) is a good approximation to the full geometrical-optics theory (7). How accurate is geometrical optics as an approximation to physical (wave) optics? To investigate this, we represent the reflected light wave ψ, with wavenumber $k = 2\pi/\lambda$ for light of wavelength λ, as a Fresnel (paraxial) diffraction integral. From the optical path length (3), and in terms of the variables (5), the integral, normalized to unity when $h(\mathbf{r}) = 0$, is

$$\psi(\mathbf{r}, Z) = -\mathrm{i}\frac{k}{\pi Z}\int\!\!\int_{\text{mirror}} \mathrm{d}\mathbf{r}' \exp\{\mathrm{i}k[(\mathbf{r}' - \mathbf{r})^2/Z - 2h(\mathbf{r}')]\}. \tag{A.1}$$

Geometrical optics emerges in the familiar way, as the large k asymptotic approximation obtained by the stationary-phase method [19], which selects the rays (6) corresponding to the values of $\mathbf{r}'$ that contribute coherently to the integral.

To investigate the quality of the approximation, we integrate (A.1) numerically, with the profile (14) corresponding to a single step. With the dimensionless variables (15), and

$$\kappa \equiv kh_0, \tag{A.2}$$

(A.1) becomes, in terms of the variable $\tau = \xi' - \xi$,

$$\psi(\xi, \zeta, \kappa) = \frac{\exp\left(-\frac{1}{4}\mathrm{i}\pi\right)}{\sqrt{\pi}}\int_{-\infty}^{\infty} \mathrm{d}\tau \exp\{\mathrm{i}[\tau^2 - \kappa\,\mathrm{erf}(\xi + \tau\sqrt{\zeta/\kappa})]\}. \tag{A.3}$$

The integral converges fast enough for convenient numerical evaluation if the contour is deformed into a complex path with $\tau = \sigma\exp(\mathrm{i}\pi/8)$ $(-\infty < \sigma < +\infty)$. Choosing $\zeta = 0.482$

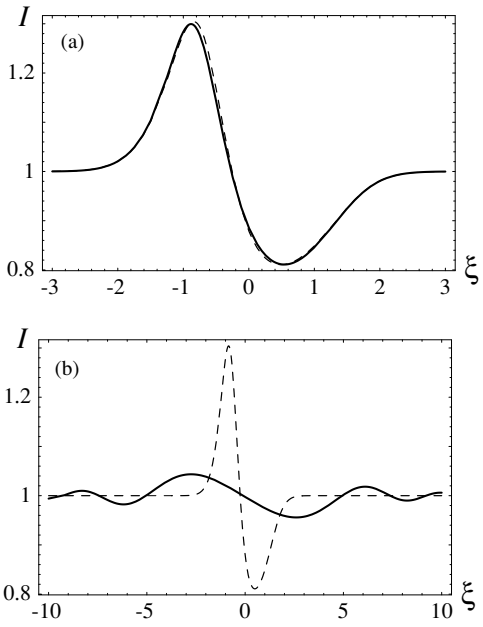

Figure 8. (a) Comparison of wave intensity $I = |\psi|^2$, computed from (A.3) (full curve) with the geometrical-optics intensity (17) (dashed curve), for the empirical values $\zeta = 0.482$, $\kappa = 3.65$. (b) As (a), with $\kappa = 0.05$, corresponding to a step height $h_0 = 5.2$ nm, and with the wave intensity computed from (A.4) (indistinguishable from (A.3) for this case).

(section 4), and representing visible light by wavelength $\lambda = 650$ nm, so that (A.2) and the height $h_0 = 378$ nm give $\kappa = 3.65$, we obtain the image shown in figure 8(a). Evidently geometrical optics is an excellent approximation.

The fact that $h_0 = 378$ nm is smaller than the wavelengths in visible light does not imply that the Laplacian image is the small-κ limit of (A.3), namely the perturbation limit corresponding to infinitely weak relief. Indeed it is not: the perturbation limit, obtained by expanding the exponential in (A.3) and evaluating the integral over τ, with a renormalized denominator to incorporate the known limit $I = 1$ for $\xi = \pm\infty$, is

$$\psi_{\text{pert}}(\xi, \zeta, \kappa) = \frac{1 - \mathrm{i}\kappa \operatorname{erf}(\xi/\sqrt{1 + \mathrm{i}\zeta/\kappa})}{\sqrt{1 + \kappa^2}}. \tag{A.4}$$

For the gentlest steps, this predicts low-contrast oscillatory images, very different from the Laplacian images of geometrical optics; this is illustrated in figure 8(b), calculated for $k = 0.05$, corresponding to $h_0 = 5.2$ nm.

References

[1] Auckland G 2001 Magic Mirrors, or Through the Looking Glass http://www.grand-illusions.com/magicmirror/magmir1.htm
[2] Ayrton W E and Perry J 1878–9 The magic mirror of Japan *Proc. R. Soc.* **28** 127–48
[3] Thompson S P 1897 *Light, Visible and Invisible* (London: Macmillan)
[4] Bragg W L 1933 *The Universe of Light* (London: G Bell)
[5] Kugimiya K 1990 'Makyoh': the 2000 year old technology still alive *J. Cryst. Growth* **103** 420–2
[6] Hahn S, Kugimiya K and Yamashita M 1990 Characterization of mirror-like wafer surfaces using the magic-mirror method *J. Cryst. Growth* **103** 423–32

[7] Tokura S, Fujino N, Ninomiya M and Masuda K 1990 Characterization of mirror-polished silicon wafers by Makyoh method *J. Cryst. Growth* **103** 437–42
[8] Shiue C-C, Lie K-H and Blaustein P R 1992 Characterization of deformations and texture defects on polished wafers of III-V compound crystals by the magic mirror method *Semicond. Sci. Technol.* **7** A95–7
[9] Swinson D B 1992 Chinese 'magic' mirrors *Phys. Teach.* **30** 295–9
[10] Yan Y-L 1992 Three demonstrations from ancient Chinese bronzeware *Phys. Teach.* **30** 341–3
[11] Mak S-Y and Yip D-Y 2001 Secrets of the Chinese magic mirror replica *Phys. Educ.* **36** 102–7
[12] Riesz F 2000 Geometrical optical model of the image formation in Makyoh (magic-mirror) topography *J. Phys. D: Appl. Phys.* **33** 3033–40
[13] Berry M V and Upstill C 1980 Catastrophe optics: morphologies of caustics and their diffraction patterns *Prog. Opt.* **18** 257–346
[14] Nye J F 1999 *Natural Focusing and Fine Structure of Light: Caustics and Wave Dislocations* (Bristol: Institute of Physics Publishing)
[15] Marr D and Hildreth E 1980 Theory of edge detection *Proc. R. Soc. B* **207** 187–217
[16] Chen J S and Medioni G 1989 Detection, localization and estimation of edges *IEEE Trans. Pattern Anal. Mach. Intell.* **11** 191–8
[17] Baraniak R G 1995 Laplacian Edge Detection http://www.owlnet.rice.edu/∼elec539/Projects97/morphjrks/laplacian.html
[18] Wolfram S 1996 *The Mathematica Book* (Cambridge: Cambridge University Press)
[19] Born M and Wolf E 1959 *Principles of Optics* (London: Pergamon)